Multiband Elliptical Patch Fractal and Defected Ground Structures Microstrip Patch Antenna for Wireless Applications

Amandeep Kaur and Praveen K. Malik*

Abstract—A multiband microstrip antenna is designed for wireless communication application with fractal and defected ground structures. Antenna prototype is fabricated using Rogers RT Duroid 5880 dielectric material on a double layer PCB with dielectric constant 2.2 and thickness 0.8 mm. Through implementing the concept of elliptical shape fractal geometry to microstrip patch antenna, more miniaturization is achieved. Further with defected ground structures, wide impedance bandwidth and gain are achieved. A compact microstrip feedline is used to couple electromagnetic energy to radiator through lumped port. Proposed antenna shows multiband characteristics. Antenna resonates at 2.6 GHz, 6 GHz, and 8.2 GHz frequency bands with impedance bandwidth of 410 MHz, 1070 MHz, and 4840 MHz. Experimental validation is done to validate simulation results. Antenna operates on different wireless standards like Wi-Fi (2.4 GHz), WLAN (2.4/5.2/5.8 GHz), Wireless Body Area Network (2.3/2.4 GHz), which falls under ISM (Industrial Scientific and Medical) band applications. It also covers communication bands, X-band (8–12 GHz) and S-band (2.3–2.4 GHz).

1. INTRODUCTION

With the tremendous growth in wireless technology, in every device data transmission is carried over wireless communication channel omitting the need of complex mesh of connecting wires as shown in Figure 1. For high speed and heavy data transmission, while maintaining the quality in multipath fading wireless environment, efficient systems are needed with compact size. Wireless technologies, like Bluetooth, LoRa, Zigbee, Wi-Fi, WI-MAX, WBAN, IoT, Mobile communication, and Satellite communication, work on specific frequency band with bandwidth requirements to carry data without any interruptions, as set by Federal Communication Commission (FCC) [1]. Antenna plays a quintessential role in wireless signal transmission, as it acts as a transducer to convert electrical signals into electromagnetic waves and vice-versa. While maintaining the compactness of wireless devices, antenna design gains much attention from researches. Antenna is a frequency dependent device and operates on a specific frequency band. So, antenna ought to be compact, cheap in cost, low weight, and as per architecture of wireless device. Antenna improves coverage and increases the data transmission capacity of wireless networks. Various types of antennas exist like Horn antenna, Long-periodic antenna, Dish antenna, Planar Inverted F-Antenna (PIFA), Dipole antenna, etc. However, microstrip patch antenna is the preferred choice due to numerous pros like compactness, lightness, affordable cost, and easy integration in wireless devices. Initially, antennas were designed to operate on single band of frequency, so to cover multiple wireless standards, multiple antennas have to be deployed in one device that further leads to bulkiness and boosts the cost. In modern communication systems, there is the need for multiband antenna with wide bandwidth and compact size. Microstrip patch antenna has narrow bandwidth but uses different techniques, and antenna bandwidth can be improved by implementing fractal and defected geometry with basic patch structure. Fractal structure
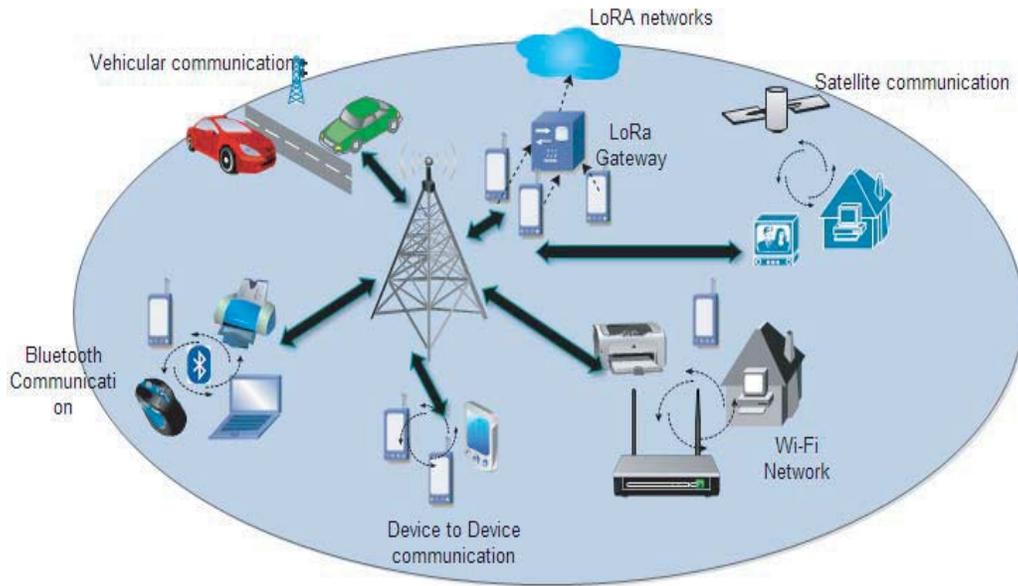
Figure 1. Wireless communication networks representation with different wireless technical standards.

is known for self-similarity and space filling characteristics, which becomes the most accepted theory in gaining antenna miniaturization [2, 3]. To implement fractal geometry, various shapes are considered like Sierpinski, Hilbert and Minkowski and these shapes are implemented in terms of iterations.

Further, these geometries are integrated with defected ground structures to improve antenna gain, reduce cross polarization, achieve good gain, and obtain wideband impedance bandwidth for microstrip antenna in wireless communication field.

In [4], fractal antenna is designed using Sierpinski geometry with aperture feed coupling method on an FR4 dielectric substrate. The antenna operates on 4.75 GHz–5.38 GHz and 6.8–7.2 GHz with bandwidths of 630 MHz and 400 MHz, respectively. The antenna covers two different UWB spectrum 4750–5280 MHz and radio astronomy frequency range from 5010 to 5030 MHz. In [5], a fractal antenna is designed using Koch snowflake geometry for wideband applications. It works on frequency bands 3.34 to 4.52 GHz, 2.2 to 3.4 GHz, and 1.45 to 4.1 GHz. In [6], a fractal antenna is designed for Wi-Fi and WiMAX applications on an FR4 dielectric substrate. It operates on 2.4 GHz to 2.48 GHz and 5.15 GHz to 5.82 GHz. The antenna size is compact, achieved using concept of fractals, but the gain is small for 2.15–3.65 dBi. In [7], a low profile fractal antenna is designed for wearable on body WBAN applications using Koch fractal geometry with a defected ground structure, and the antenna operates from 2.36 GHz to 2.55 GHz with the gain of 2.06 dBi. In [8], a multiband fractal circular patch antenna is presented which is designed on an FR4 substrate, operates from 2.93 GHz to 9.53 GHz, and is suitable for UWB, S- and C-band applications. A super wideband fractal wideband antenna using a CPW-fed antenna is presented. The antenna is proposed on an FR4 substrate material with rectangular notches on ground. The proposed structure operates from 3.8 GHz to 68 GHz and is suitable for UWB applications [9].

Defected ground structures concept is used in [10] with a Zigzag-shaped patch structure. The proposed antenna operates on three resonant frequencies, 2.45 GHz, 5.28 GHz and 3.5 GHz for WLAN and WiMAX applications. Defected ground structure concept is used in [11] to achieve circular polarization. In the ground plane by further adjusting the dimensions of etched Fractal Defected Ground Structures (FDGSs), circularly polarized (CP) radiations can be obtained. Impedance bandwidth achieved using this method is 30 MHz, and the antenna resonates from 1.558 to 1.588 GHz and 5.15 dBi AR bandwidth is 6 MHz from 1.572 to 1.578 GHz with gain from 1.7 and 2.2 dBi. In [12], a U-shaped fractal geometry is integrated with a DGS to improve antenna gain and efficiency by restoring radiation patterns. The antenna is fabricated using a Taconic CER-10 substrate with dimensions 83 mm × 45 mm and thickness 3.18 mm, and dielectric constant $\varepsilon r = 10$. The overall size of the antenna

is $100 \times 100 \times 3.18$ mm. Three iterations of U-shaped structures are used. Results are calculated using HFSS software. Antenna resonates at 45 MHz frequency band. Gain of the antenna is calculated with and without using FDGS. The gain without FDGS is 2.56 dBi and with FDGS is 5.38 dBi.

2. ANTENNA DESIGN

A planar microstrip patch antenna consists of a top layer called patch, a bottom layer known as ground layer, and a dielectric substrate sandwiched between the two. These Planar Microstrip Patch Antennas (PMPAs) can be designed by etching different structures like square, circle, ellipse, E, H, S, etc. on copper layers of a double-side PCB. The top patch layer acts as a radiator for transmitting antenna and a receptor for receiving antenna, whereas the bottom PCB layer acts as ground plane which can be a plane surface or defected one [13]. In Microstrip Patch Antenna (MPA), antenna radiations occur due to fringing effect between corners of the designed patch structure and the ground plane. Patch antenna can use different geometries to obtain resonant frequency bands for desired applications. These days elliptical patch antennas are gaining much attention due to their circular polarization characteristics among different patch structures. For today's wireless communication systems, broadband and multiple features requirement can be only fulfilled by elliptical patch fractal antennas [14].

Figure 2 shows the proposed multiband antenna design for wireless applications. The proposed structure is designed using a Rogers RT Duroid 5880 substrate material with thickness ($t = 0.8$ mm), dielectric constant ($\varepsilon r = 2.2$), and loss tangent 0.0009. The RT Duroid substrate dimensions are $50\,\text{mm} \times 50\,\text{mm} \times 0.8\,\text{mm}$ with an elliptical shape patch. To obtain impedance matching lumped port with 50-ohm resistance is used with Y-axis and Z-axis with dimensions of 3.87 mm and 0.8 mm, respectively, and microstrip feed method is used for antenna feeding with dimensions 12.94 mm $\times$ 3.87 mm. To achieve more compactness in antenna design an elliptical patch with $n = 3$ iterations is used, without changing the physical length of antenna to obtain multiband characteristics of the proposed antenna structure. The radiator or receptor element of proposed antenna is the fractal elliptical shape patch structure which is fed by a microstrip feed line. In the proposed design, each ellipse with different radii is designed to operate on a specific frequency to exhibit multiband characteristics for this antenna architecture. The smallest inner ellipse resonates at high frequency bands due to its small radiation area, whereas the largest outer ellipse operates at low frequency bands due to its large surface resonating area. The remaining ellipse resonates between low cutoff and high cutoff frequencies to obtain wide band characteristics.

Defected ground plane is used to improve antenna performance parameters like bandwidth, gain, and to suppress cross polarization. These structures are used to divert current distribution in ground plane to change the inductive and capacitive properties of proposed antenna. Defected ground dimensions considered are 12.7 mm $\times$ 50 mm $\times$ 0.8 mm. Figures 2(a) to (c) show the proposed fractal shapes with different iteration orders. Fractal curves are characterized by two parameters: indentation factor (IF) and iteration order (IO). All of these antennas are fabricated on 0.8-mm substrates with relative permittivity 2.2 and are matched by quarter wavelength transformers. The radius of elliptical patch changes with the number of iterations. As in the proposed antenna design, the number of iterations increases, and the electrical length of antenna patch structure also increases without changing the overall antenna dimensions, thus different resonant bands are achieved for the proposed antenna. Finally, the proposed antenna with total iteration is obtained as shown in Figure 2(c) and simulated in HFSS software. The back view of proposed antenna is given in Figure 2(d) and elaborated view in Figure 3. The proposed antenna patch and defected ground dimensions are considered as mentioned in Table 1. Antenna defected ground plane consists of a rectangle with a triangle on top of it, and the complete structure has three steps cut from the center of ground plane with vertical step sizes $r1$, $r2$, and $r3$ of 1 mm and horizontal step size $s1$, $s2$, and $s3$ of 0.77 mm with proper calculation as shown in Figure 4. These steps are basically called the capacitive step cuts to achieve wideband characteristics of the proposed antenna by reducing inductance or act as inductance counteraction.

To understand the working of proposed antenna in more detail, antenna current distribution analysis can be done, and electric current distribution density can be observed in HFSS simulator by varying different frequencies of operation over different values of phi and theta to investigate the return loss behavior of proposed structure. Electric and magnetic field density plots for the designed antenna
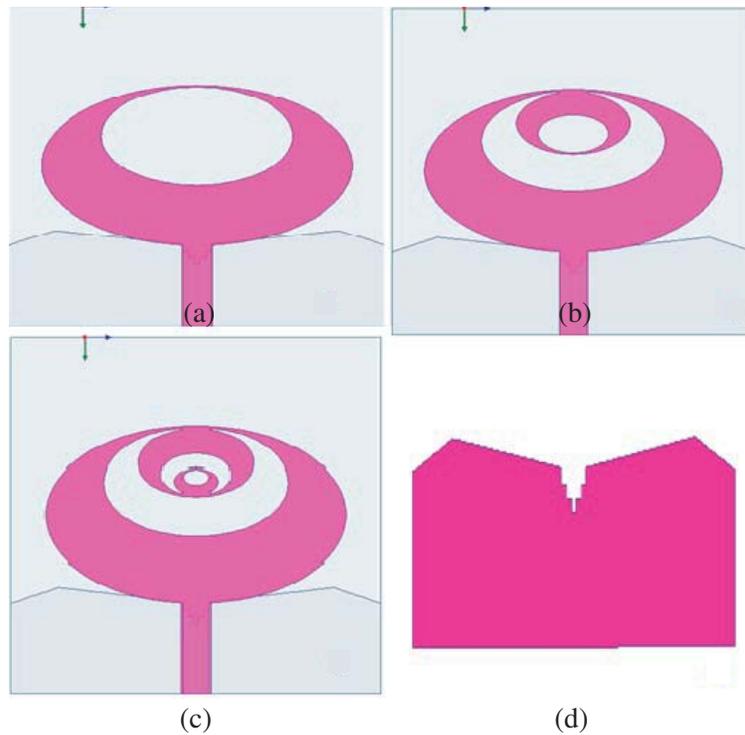
Figure 2. Multiband Elliptical Shaped Fractal and Defected Antenna. (a) Iteration-1 ($n = 1$). (b) Iteration-2 ($n = 2$). (c) Iteration-3 ($n = 3$). (d) Defected Ground (Back view).
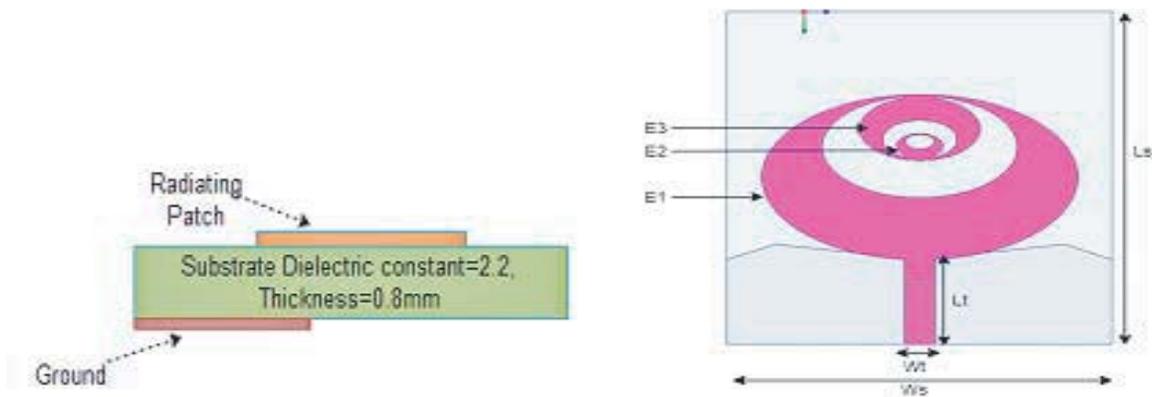

Figure 3. Proposed Antenna top dimensions and defected ground.

at resonant frequencies are demonstrated in Figure 5. It is depicted that the maximum current is concentrated along the edges of feedline, at the edges of the elliptical patch structure and the edges of ground plane which is responsible for obtaining multiband and wide bandwidth characteristics for the proposed antenna. Also, current is distributed uniformly along the surface of elliptical patch and defected ground plane. The current distribution across edges of patch, feedline, and defected ground increases its electrical length which is responsible for antenna to resonate at 2.33 to 2.74 GHz, 5.46 to 6.53 GHz, and 7.60 to 12.44 GHz frequency bands with good return loss values.

3. ANTENNA SIMULATION RESULTS

Antenna performance can be analyzed by its radiation and return loss properties. Scattering parameters or reflection parameters determine how antenna is capable to radiate and receive power. Antenna radiation properties provide information related to antenna directivity, gain, and density of power for frequency bands over which the antenna resonates. These parameters can be represented in terms
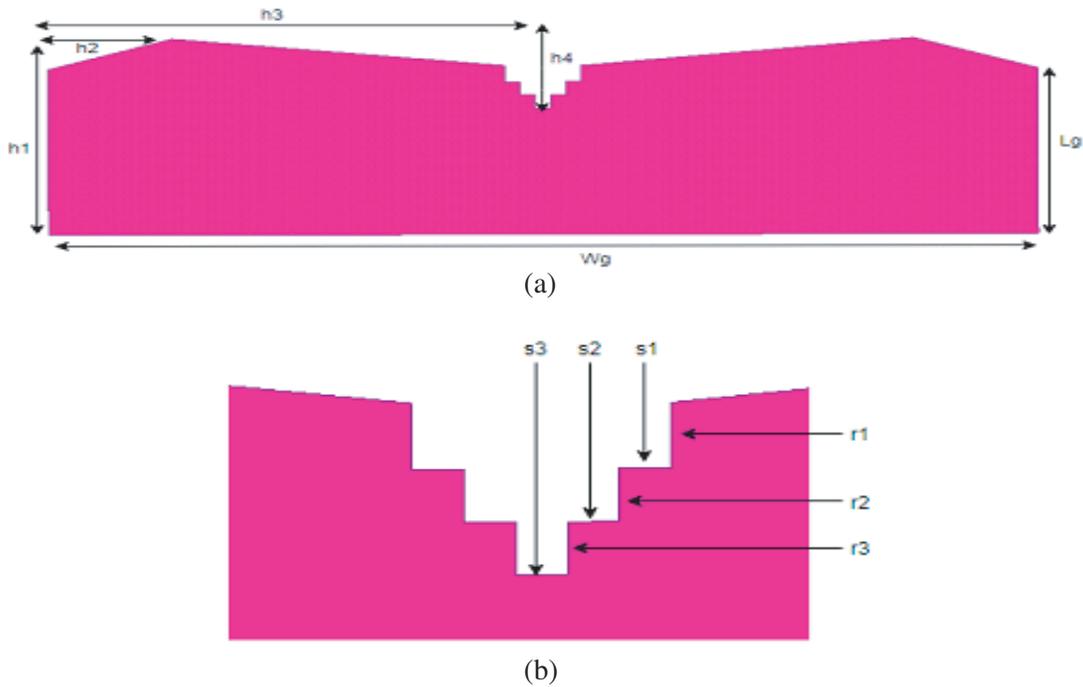

(a)

(b)

Figure 4. Proposed Antenna top dimensions. (a) Proposed Antenna defected ground: Back view. (b) Defected ground stair cuts elaborated view.
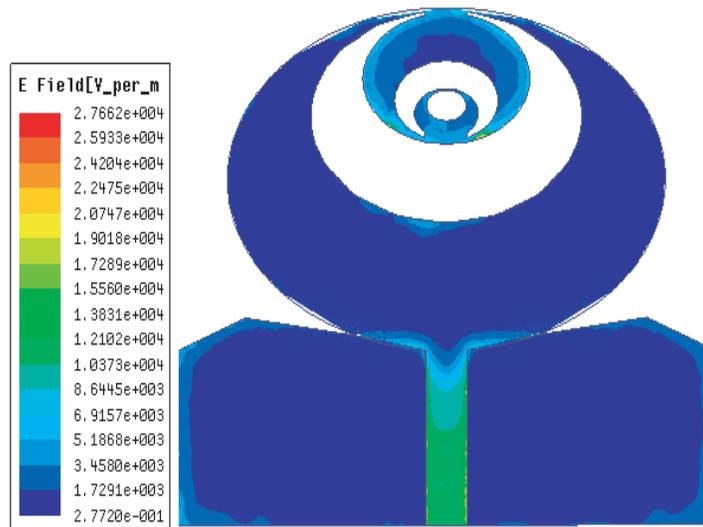

Figure 5. HFSS Simulation E-field distribution of proposed microstrip patch antenna.

of 2-D or 3-D graphical patterns. To analyze antenna performance, simulation is carried out using HFSS simulator from 1 GHz to 15 GHz prior fabrication using PCB technology. Antenna performance is evaluated in terms of return loss, bandwidth, voltage standing wave ratio (VSWR), and radiation pattern as shown in Table 2.

Figure 6 shows the reflection coefficient summated performance of the proposed antenna. It is

Table 1. Dimensions of proposed elliptical shaped patch multiband fractal and defected ground antenna.

| Parameters	Dimensions (mm)
Substrate used	Rogers RT Duroid 5880
Substrate thickness (h)	0.8 mm
Dielectric constant (εr)	2.2
Ls (Substrate Length)	50
Ws (Substrate Width)	50
Lt (Transmission line length)	12.94
Wt (Transmission line Width)	3.87
$E1$ (Ellipse 1)	12.42
$E2$ (Ellipse 2)	4.74
$E3$ (Ellipse 3)	1.81
Lg (Ground length)	12.7
Wg (Ground Width)	50
$r1, r2, r3$ slots	1
$s1, s2, s3$ slots	0.77
$h1$	15.03
$h2$	6.25
$h3$	23.06
$h4$	5.33
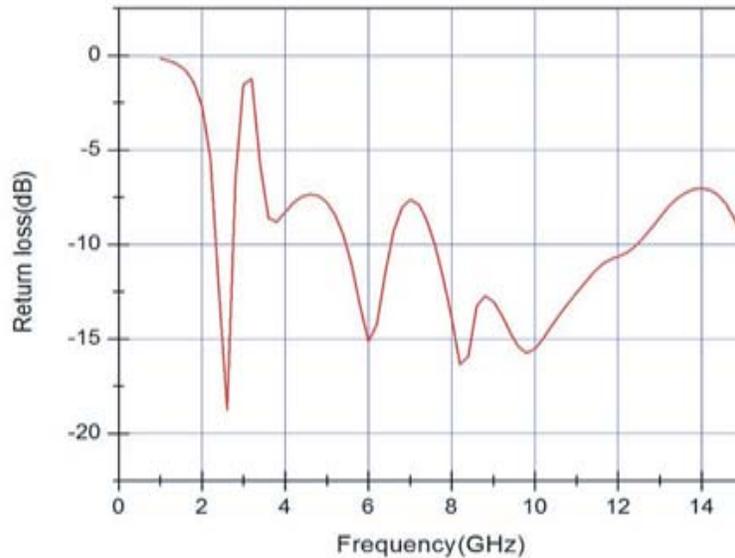
Figure 6. Simulated Return loss performance for multiband Elliptical patch antenna.

Table 2. Proposed antenna simulated results in terms of S_{11}, gain, VSWR and bandwidth.

Frequency (GHz)	Cut off frequency	Return loss (dB)	Bandwidth (MHz)	VSWR	Gain (dBi)
2.33–2.74	2.6	−18.18	410	1.2	5.42
5.46–6.53	6	−15.11	1070	1.4	6.52
7.60–12.44	8.2	−16.33	4840	1.35	7.67

depicted from the graph that the proposed antenna shows multiband characteristics with wide-band impedance bandwidth. Antenna resonates over three frequency bands with operating frequencies 2.6 GHz, 6 GHz, and 8.2 GHz with return loss values −18.18, −15.11 and −16.33 dB, respectively. Impedance bandwidths achieved over respective bands of operation are 14.96% (2.33–2.74), 16.38% (5.46–6.53 GHz), and 38.90% (7.60–12.44 GHz), respectively. For achieved frequency bands of operation VSWR performance is less than 2, which is acceptable, and its value should be between 1 and 2 practically. VSWR plot is given in Figure 7.
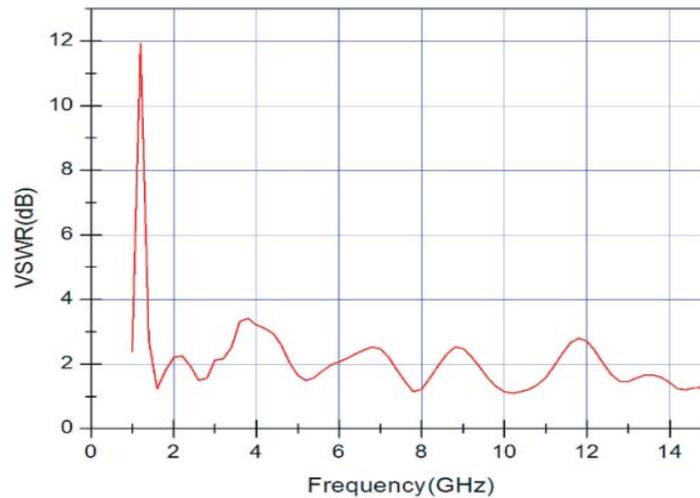

Figure 7. Simulated VSWR vs frequency performance for multiband Elliptical patch antenna.

Figure 8 shows the simulated gain performance of proposed antenna. The gain for frequency band 2.33 GHz to 2.74 GHz varies between 4.91 dBi and 5.86 dBi. Gain variation is depicted from 6.12 dBi to 5.84 dBi for frequency band of operation 5.4 GHz to 6.6 GHz and 7.71 dBi to 7.75 dBi for 7.6 GHz to 12.4 GHz frequency band of operation. It is observed that the antenna gain for proposed structure is less on low frequencies and comparatively more at high frequencies as given in Figure 8. Maximum gain achieved is between frequencies 10 GHz and 12 GHz.

Far field radiation patterns for the proposed antenna in terms of 3-D polar gain plot for proposed antenna at obtained resonant frequencies 2.6 GHz, 6 GHz, and 8.2 GHz are represented in Figure 9. The proposed antenna exhibits high gains of 5.42 dBi, 6.52 dBi, and 7.67 dBi, respectively, at these operating frequencies. 2-D radiation pattern for the proposed antenna is given in Figure 10 at Phi-0 and Phi-90 degrees for resonating frequencies 2.6 GHz, 6 GHz, and 8.2 GHz in E-plane and H-plane.

For frequencies 2.6 GHz and 6 GHz, radiation beamwidth is large as compared to 8.2 GHz in azimuth plane (H-plane) as shown in Figure 10. Radiation pattern achieved shows semi-omnidirectional characteristics. For Phi = 90 degrees, at frequency 2.6 GHz radiation pattern achieved is omnidirectional, i.e., the proposed antenna at lower frequencies radiates in all directions with the gain of 5.42 dBi. For resonant frequency 8.2 GHz, the antenna radiates between 30 degrees and 150 degrees
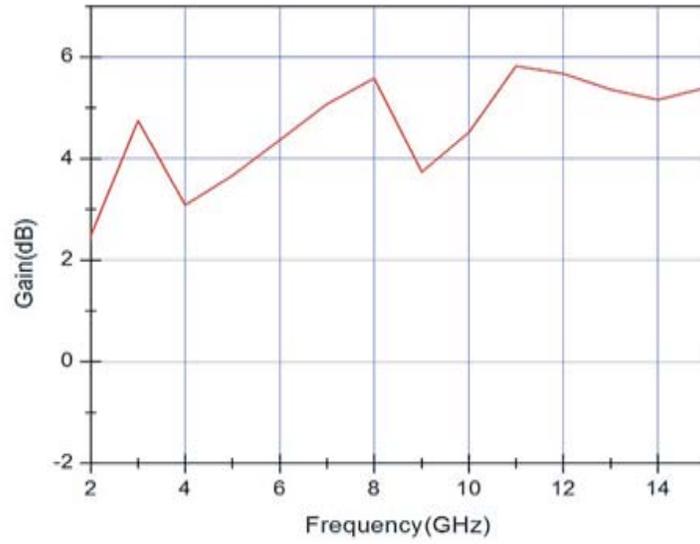
Figure 8. Simulated Gain vs frequency performance for multiband Elliptical patch antenna.
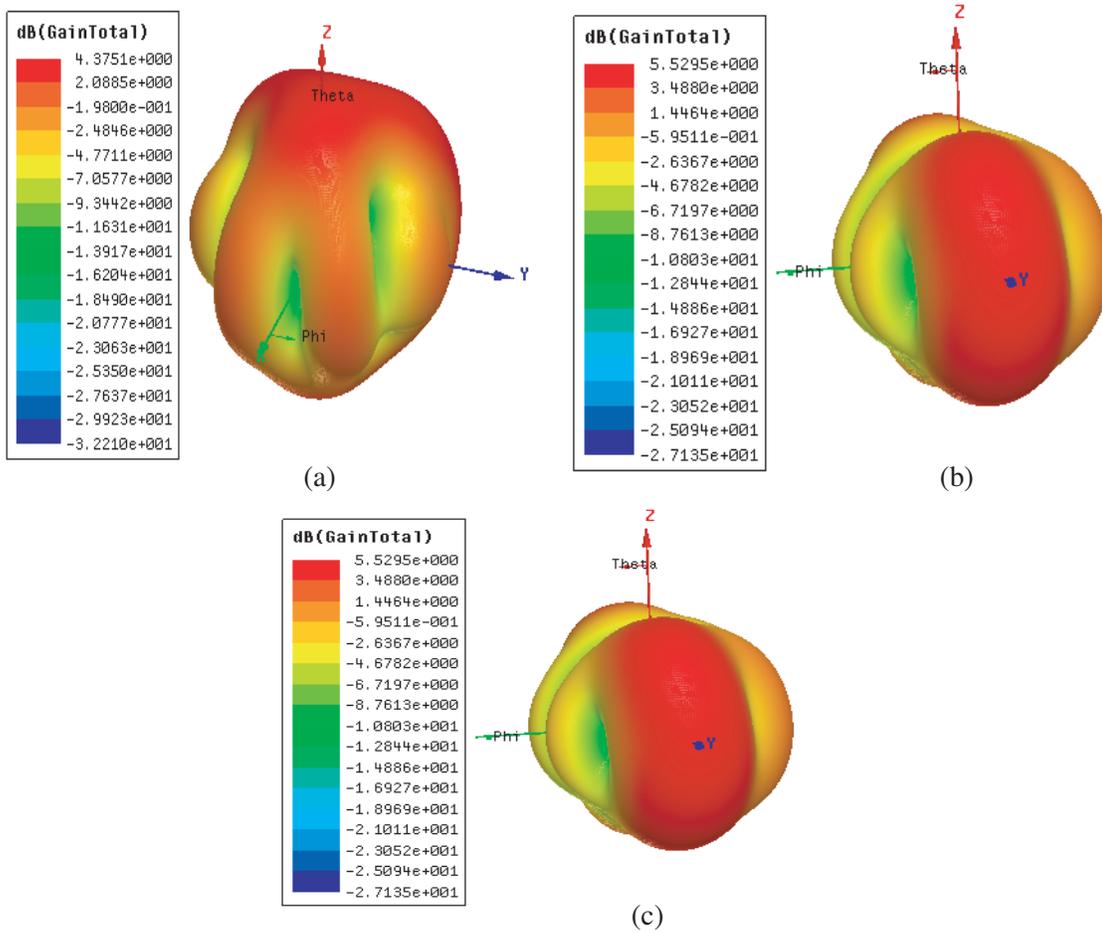

(a)

(b)

(c)

Figure 9. Simulated 3-D polar gain plot for proposed Elliptical patch multiband band fractal and defected antenna. (a) 3-D Gain plot at 2.6 GHz. (b) 3-D Gain plot at 6 GHz. (c) 3-D Gain plot at 8.2 GHz.
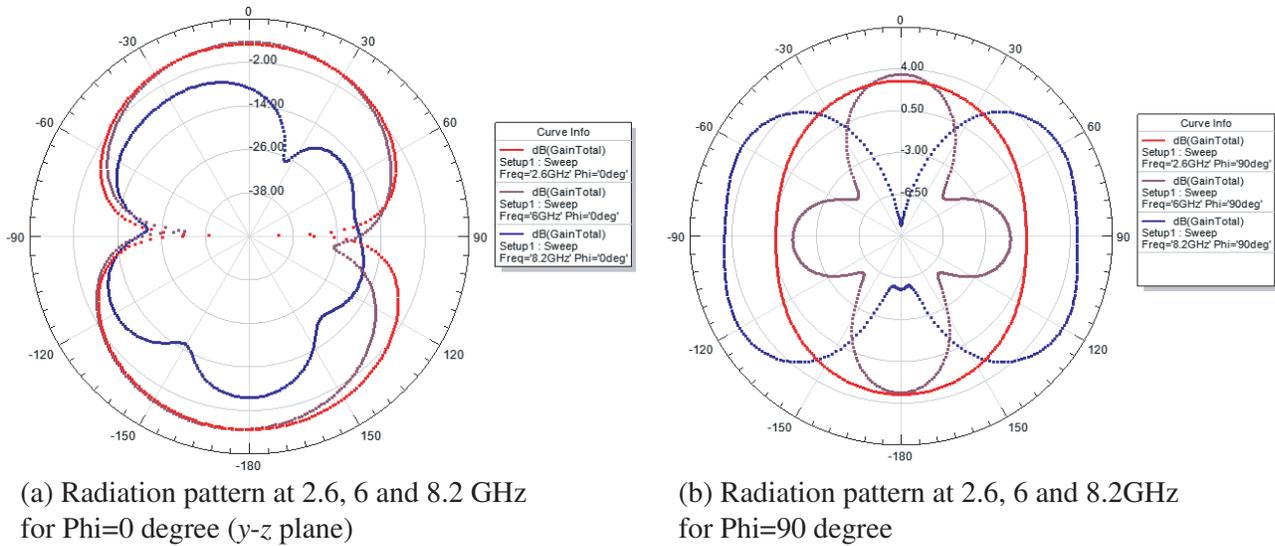
(a) Radiation pattern at 2.6, 6 and 8.2 GHz for Phi=0 degree (*y-z* plane)

(b) Radiation pattern at 2.6, 6 and 8.2GHz for Phi=90 degree

Figure 10. Radiation patterns at 2.6 GHz, 6 GHz and 8.2 GHz for (a) phi = 0-degree, (b) Phi = 90 degree.

with the gain of 7.67 dBi, and at 6 GHz major lobs are obtained at theta = 0 and −180 degrees with minor lobs on 90 and −90 degrees.

4. ANTENNA FABRICATION

After performing simulations of the proposed antenna in HFSS, antenna prototype is fabricated on a Roger RT Duroid 5880 Double layer PCB with copper thickness of 0.35 micrometers as represented in Figure 11. The fabricated antenna is fed using a microstrip feedline through a 4 hole flange Sub-Miniature Version A (SMA) connector by Amphenol consisting of brass and gold plated with 50-ohm resistance and gives excellent performance between 0 and 18 GHz frequency band of operation with temperature tolerance capability −55°C ∼ +155°C.

Return loss and VSWR of the fabricated antenna are measured using Vector Network Analyzer

Figure 11. Top view of proposed fabricated Elliptical patch Multiband band fractal and defected antenna.
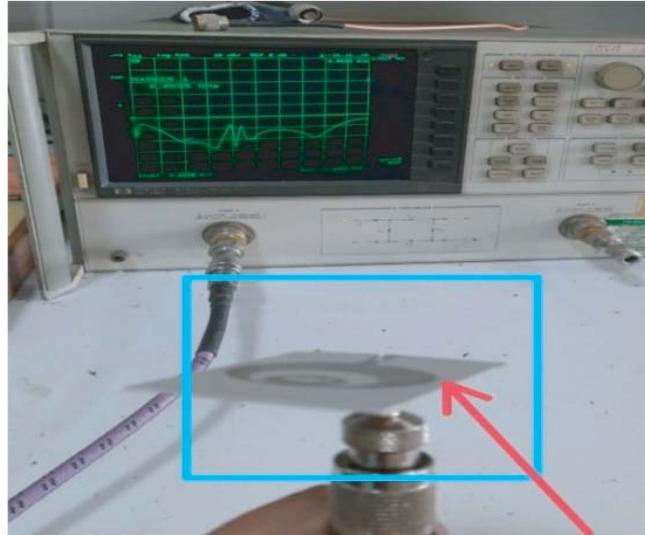
Figure 12. Return loss Measurement Setup used for Experimental analysis for proposed Elliptical patch Multiband band fractal and defected antenna.

HP-8720A with frequency band of operation from 1 GHz to 15 GHz. Before return loss measurement, VNA is calibrated using Calibration Kit. Figure 12 shows the antenna measurement setup for return loss measurement.

For the proposed antenna, simulated and measured return loss performances are given in Figure 13. It is evident from the graph that simulated and measured impedances agree with each other. From tested return loss characteristic, the proposed antenna resonates between 2.2 GHz and 13.2 GHz which shows antenna wideband characteristics. From Figure 13, it is clear that resonant frequency bands achieved with impedance bandwidth from measured results are 2–2.2 GHz (9.09%), 3.2–6.8 GHz (52.9%), 7–7.7 GHz (9.09%), and 7.74–13.2 GHz (41.36%).

Some mismatch and discrepancies are observed between simulated and measured results at lower frequencies due to fabricated errors, cable loss, scattering measurement environment, and SMA
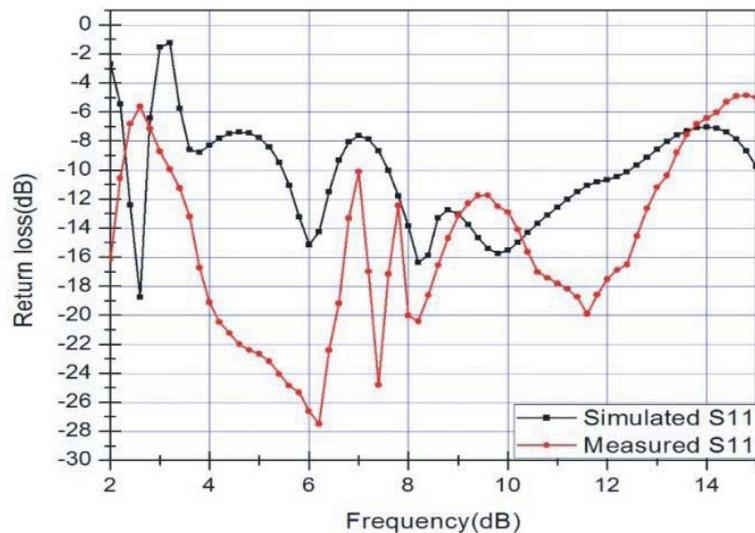

Figure 13. Simulated and Measured Return loss plot for proposed Elliptical patch Multiband band fractal and defected antenna.
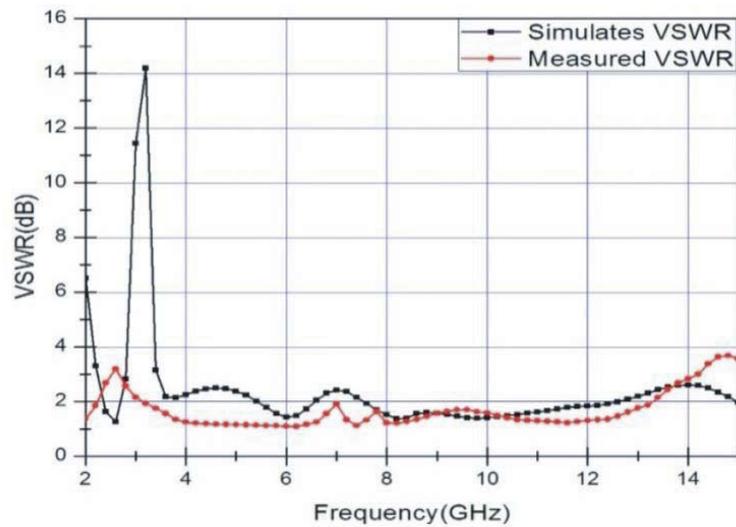
Figure 14. Simulated and Measured VSWR performance for proposed Elliptical patch Multiband band fractal and defected antenna.

connector quality, but at the end impedance bandwidth is maintained which is the main objective of this research. Also, the plot for simulated and measured VSWRs is given in Figure 14, and they are in good agreement except for low frequency below 2.6 GHz, where simulated VSWR performance does not agree with measured results. Simulated VSWR value is high, but practically for lower frequencies measured VSWR performance is acceptable.

5. ANTENNA GAIN AND RADIATION PATTERN MEASUREMENTS

Figure 15 shows the simulated and measured gain performances for the proposed antenna. Antenna gain measurement is carried out using reference method. To measure the gain in far field environment of the proposed antenna, initially a proper distance is calculated using a far field formula for reference antenna and AUT (proposed antenna). Reference antenna considered is a Log Periodic Dipole Antenna
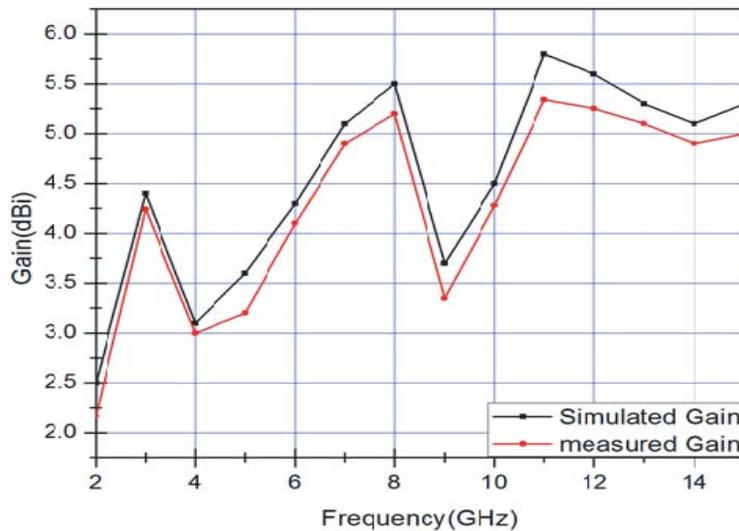

Figure 15. Simulated and Measured Gain for proposed elliptical shaped patch multiband antenna.

(LPDA). The proposed antenna gain measurement is done by using Wiltron 68147B Signal Generator and HP-8593E Spectrum analyzer. It is depicted from the graph that simulated and experimental gain results are in good greement with each other for the complete operating range of frequencies and more than 2 dB. For the fabricated antenna, the values of measured gain achieved are 4.92, 5.97, and 7.35 dBi at 2.6 GHz, 6 GHz, and 8.2 GHz, respectively, which are practically acceptable gains for wireless communication applications.

Figures 16(a) to (c) show the simulated and measured radiation patterns at 2.6 GHz, 6 GHz, and 8.2 GHz in E-plane and H-plane. Radiation pattern measurement setup used is the same as gain measurement. The proposed fabricated antenna is placed in far field region with respect to reference antenna and aligned properly. Radiation pattern for the proposed antenna achieved at 2.6 GHz and
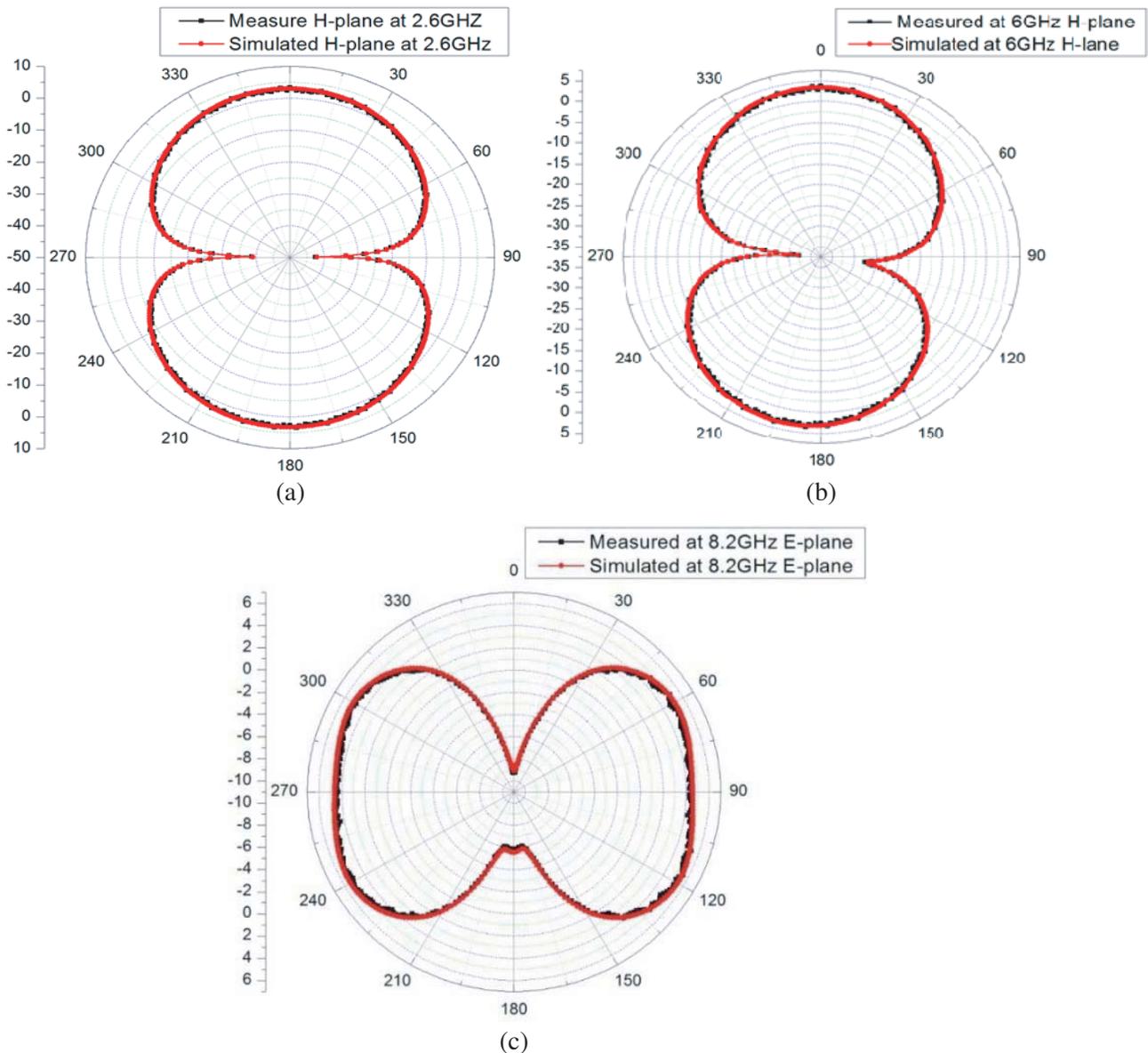
Figure 16. Simulated and Radiation pattern for different resonating frequencies. (a) Measured and Simulated radiation pattern at 2.6 GHz in H-plane for proposed antenna. (b) Measured and Simulated radiation pattern at 6 GHz in H-plane for proposed antenna. (c) Measured and Simulated radiation pattern at 8.2 GHz in E-plane for proposed antenna

6 GHz in dumb-bell shaped semi-omnidirectional in H-plane (y-z plane) and at frequency 8.2 GHz is also semi-omnidirectional in E-plane (x-z) at phi = 90 degrees.

6. PARAMETRIC ANALYSIS

The proposed antenna patch, ground, and substrate dimensions are calculated using mathematical expression defined in antenna modelling to operate antenna on the desired frequency band of operation. Antenna performance is also analyzed and compared in terms of some parameters like by changing the substrate thickness for Rogers RT Duroid 5880 and by considering FR4 substrate material. Different substrate thicknesses (t) considered are 0.5, 0.8, and 1.6 mm.

6.1. Effect of Substrate Material

Return loss performance of the proposed antenna is analyzed using two substrate materials, which are easily available in market, FR4 and Rogers DT Duroid 5880 with thickness $t = 0.8$ mm. It is depicted from Figure 17 that Rogers RT Duroid 5880 S_{11} performance is better than FR4 with the same thickness. As shown in Figure 17, the return loss value of RT Duroid is below -10 dB for lower frequencies from 2.33 to 2.74 GHz with S_{11} value -18.18 dB at cutoff frequency 2.6 GHz, but for FR4 dielectric substrate, S_{11} values from 1 to 5 GHz are not below -10 dB. For FR4 dielectric substrate of the proposed antenna, good bandwidths of 1.7 GHz and 2.91 GHz are obtained from 6.43–8.2 GHz and 12.09–15 GHz frequency bands, respectively. The return loss value for RT Duroid is below -10 dB from 7.6 GHz to 12.4 GHz frequency band that gives wide-band impedance bandwidth of 4.8 GHz. So, it is analyzed that the proposed antenna results are good at both lower and higher cuts of frequencies with Rogers RT Duroid as compared to FR dielectric substrate material in terms of bandwidth.
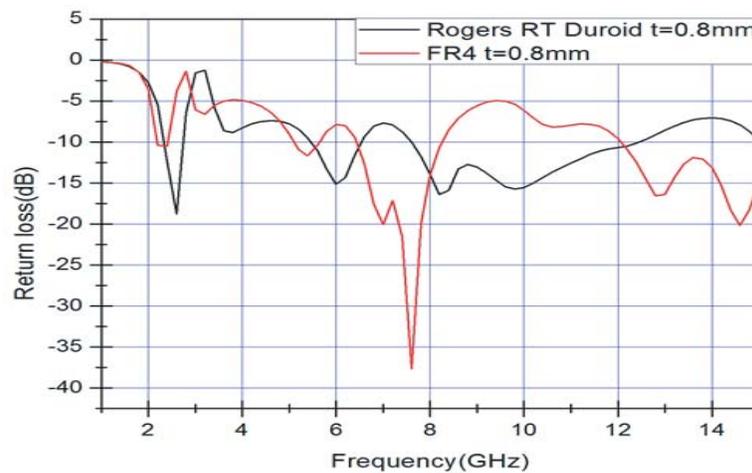

Figure 17. Proposed antenna S_{11} performance with Rogers and FR4 dielectric substrate material with thickness 0.8 mm.

6.2. Effect of Substrate Thickness

Substrate selection to obtain the desired antenna performance is quintessential. It provides mechanical strength to antenna structure and affects the electrical properties of antenna as surface wave formation occurs in antenna which extracts the total power for free space. For the proposed antenna effect of change in dielectric height is observed on return loss performance. Dielectric thickness $t = 0.5$ mm, 0.8 mm, and 1.6 mm is considered for Rogers RT Duroid 5880, and performance is compared in terms of S_{11} parameter as shown in Figure 18. The proposed antenna shows good S_{11} performance with dielectric thickness 1.6 mm as compared to 0.8 mm and 0.5 mm, but for the antenna with a dielectric
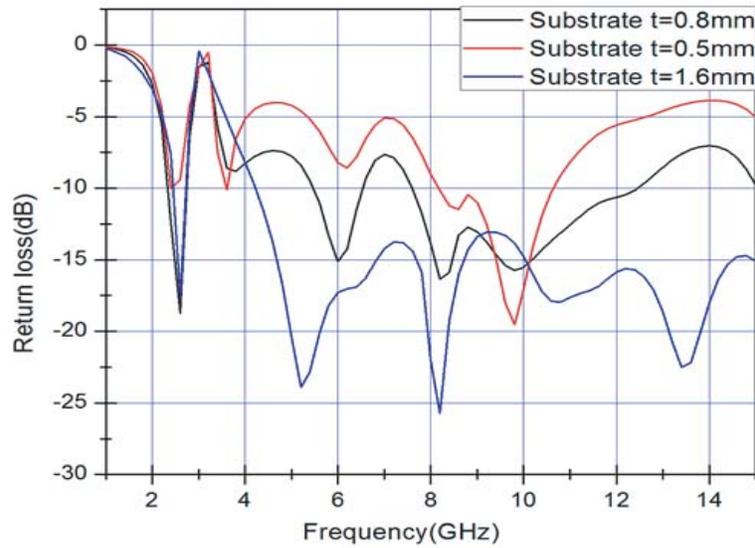
Figure 18. Proposed antenna S_{11} performance with different substrate height with Rogers RT Duroid 5880 material.

substrate of 0.8 mm thickness is used to achieve compactness in design and for the easy integration of antenna structure for wireless devices.

6.3. Effect of Iterations

Figure 19 represents the effect of different iterations on return loss performance for the proposed antenna. It is depicted from Figure 19 that with the increase in iteration, the return loss coefficient value increases, and the effect on bandwidth is also analyzed. The return loss performance of proposed antenna is better over lower frequencies and higher frequencies than Iteration-1 and Iteration-2. Also, Iteration-2 and Iteration-3 perform better over high frequency bands from 7.6 GHz to 12.4 GHz.
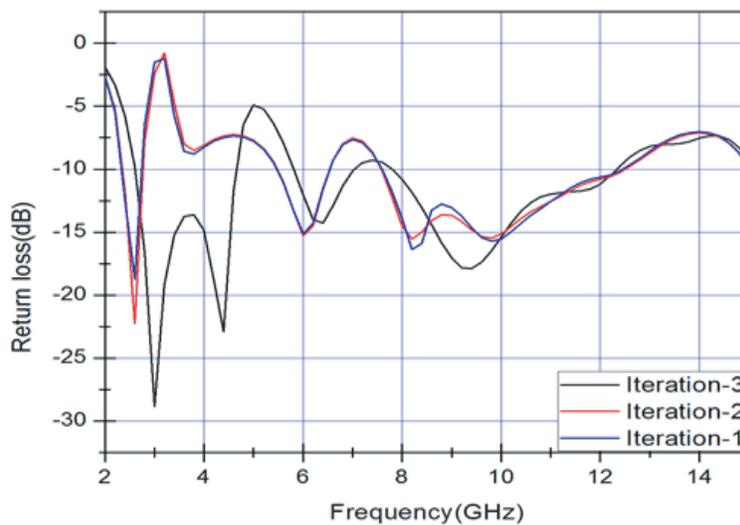

Figure 19. Effect of different Iterations on return loss performance for [proposed Elliptical patch Multiband band fractal and defected antenna.

Performance comparison analysis of the proposed antenna is carried out with existing antennas in literature in following Table 3 in terms of overall antenna dimensions, achieved frequency band of operation, gain, and bandwidth.

Table 3. Proposed antenna performance comparative analysis with existing antenna.

Ref. No.	Ant. Dimensions (mm)	Substrate used	Operating Frequency (GHz)	Bandwidth (MHz)	Gain(dBi)	Remarks
[15]	60 × 60 × 4.8	FR4 (two layers)	4.75–5.38, 6.8–7.2	630, 400	5.85, 9.5	Large in size and use two layers of substrate
[16]	110 × 110 × 6.6	FR4 (3 layers)	0.911–0.933, 2.40–2.57	20, 170	0.8, 5.9	Large dimensions, less bandwidth
[17]	138 × 90 × 6.79	Roger RT Duroid 5870	1.387–1.696	309	5.62–6.6	Large dimensions, single band
[18]	100 × 100 × 11	Rogers RT Duroid 5880	1.4–1.6, 2–2.4	20, 40	2.3, 6	Very small bandwidth and large dimensions
[19]	60 × 88 × 4.8	FR4	3.62–4.75	1130	3.4	Height is large
[20]	96 × 73 × 14	RO4003C	2.5–2.7, 3.4–3.6	30, 20	9.2, 7.0	Large dimensions, small bandwidth
[21]	95 × 60 × 0.8	FR4	0.74–0.965, 1.380–2.703	225, 323	0.76–4.5	Large dimension, less gain
[22]	45 × 45 × 3.18	FR4	(1.558–1.588), (1.572–1.578)	30, 6	1.7–2.2	Less BW and gain, use large dielectric constant ($\varepsilon = 10$)
[23]	80 × 40 × 1.58	FR4	2.2–3.4, 3.34–4.52, 1.45–4.1	1120, 1180, 2650	2.2–2.4	Wideband, small gain and large dimensions
[24]	50.8 × 62 × 0.8	FR4	1.3–20	19700	8	Very complex structure, large dimensions and single wideband
[25]	55 × 48 × 0.58	Rogers RT Duroid 5880	2.34–2.56	220	2.36	Small, gain and bandwidth, large dimensions, single band
[26]	100 × 100 × 3.18	Taconic CER-10 ($\varepsilon r = 10$)	45	–	2.56 (without DGS), 5.38 (with DGS)	Large dimensions, complex structure, high dielectric constant
[27]	100 × 100 × 3.18	Taconic CER-10	1.55–1.6	45	2.38	Small gain and bandwidth, large dimensions
[28]	150 × 150 × 4	Jeans Fabric	1.78–1.98, 2.38–2.505	200, 125	—	Small bandwidth, large in size
[29]	59.5 × 59.9 × 3.7	Fabric	2.4–2.48	80	3.8	Small bandwidth
[30]	88 × 20 × 1.6	FR4	1.980–2.010, 3.40–3.50, 4.94–4.99, 6.0–6.8	30, 100, 50, 80	3.23, 4.3, 5.95, 4.65	Small bandwidth, large dimensions
[31]	56 × 44 × 0.80	FR4	1.7–2.92, 2.92–4.28, 5–5.98, 6.37–6.78, 7.33–8	1.22, 1.36, 0.98, 0.41, 0.67	5.28	Small bandwidth
[32]	60 × 30 × 1.6	FR4	2.4–2.5, 5.725–5.875	100, 150	2.2	Less Gain and bandwidth
Proposed	50 × 50 × 0.8	**Rogers RT Duroid**	**2.33–2.74, 5.46–6.53, 7.60–12.44**	**410, 1070, 4840**	**5.42, 6.52, 7.67**	Wide bandwidth, compact structure and good gain

7. CONCLUSION

In this article, a compact, low profile, elliptical patch multiband fractal microstrip patch antenna with slotted ground plane is presented, and the performance is verified with the help of experimental analysis. Parametric analysis is done on the proposed antenna by varying substrate thickness and changing dielectric substrate material from Rogers RT Duroid to FR4. It is analyzed that antenna performance is good for Roger RT Duroid with 0.8 mm thickness. The antenna's simulated and measured results are in good agreement with each other. It resonates on three different frequencies 2.4, 6, and 8.2 GHz with bands 2.33–2.74, 5.46–6.53, 7.60–12.44, and impedance bandwidths achieved are 410, 1070, and 4840 MHz, respectively. The proposed antenna shows wideband and multiband characteristics. Comparative analysis of the proposed antenna is carried out with existing antenna in terms of gain, bandwidth, and dimensions. The antenna is compact and provides large bandwidth over other antenna structures. Owing to these advantages, the antenna is a good candidate for wireless communication applications.

REFERENCES

1. International Telecommunication Union, Radio Communication Study Groups, "Framework for the introduction of devices using ultra-wideband technology," Document 1/85 (Rev. 1)-E, 09, Nov. 2005.

2. Mandelbrot, B. B., *The Fractal Geometry of Nature*, W. H. Freeman and Company, San Francisco, 1982.

3. Shahu, B. L., S. Pal, and N. Chattoraj, "Design of super wideband hexagonal-shaped fractal antenna withtriangular slot," *Microwave and Optical Technology Letters*, Vol. 57, No. 7, 1659–1662, 2015.

4. Kaur, A., R. Khanna, and M. V. Kartikeyan, "A stacked Sierpinski gasket fractal antenna with a defected ground structure for UWB/WLAN/Radio astronomy/STM link applications," *IEEE Letters on Microwave and Optical technology*, Vol. 57, 2786–2792, 2015.

5. Choukiker, Y. K. and S. K. Behera, "Wideband frequency reconfigurable Koch snowflake fractal antenna," *IET Microw. Antennas Propag.*, Vol. 11, No. 2, 203–208, Feb. 2017.

6. Abed Sahab, A., M. Singh, and M. Islam, "Compact Fractal antenna circularly polarized radiation for Wi-Fi and WiMAX communications," *IET Microwaves Antennas & Propagation*, Article. 10.1049/iet-map.2018.5213.

7. Arif, A., M. Zubair, M. Ali, M. U. Khan, and M. Q. Mehmood, "A compact, low-profile fractal antenna for wearable on-body WBAN applications," *IEEE Antennas and Wireless Propagation Letters*, Vol. 18, No. 5, 981–985, May 2019.

8. Gupta, M. and V. Mathur, "Wheel shaped modified fractal antenna realization for wireless communications," *AEU, International Journal of Electronics and Communications*, Vol. 79, 257–266, June 13, 2017.

9. Singhal, S. and A. K. Singh, "CPW-fed octagonal super-wideband fractal antenna with defected ground structure," *IET Microwaves, Antennas & Propagation*, Vol. 11, No. 3, 370–377, 2017.

10. Sanjeeva Reddy, B. R. and D. Vakula, "Compact Zigzag-shaped-slit microstrip antenna with circular defected ground structure for wireless applications," *IEEE Letters on Antennas and Wireless Propagation*, Vol. 14, 678–681, 2015.

11. Wei, K., J. Y. Li, L. Wang, R. Xu, and Z. J. Xing, "A new technique to design circularly polarized microstrip antenna by fractal defected ground structure," *IEEE Transactions on Antennas and Propagation*, Vol. 65, No. 7, 3721–3725, 2017.

12. Wei, K., B. Zhu, and M. Tao, "The circular polarization diversity antennas achieved by a fractal defected ground structure," *IEEE Access*, Vol. 7, 92030–92036, 2019.

13. Balanis, C. A., *Microstrip Antennas, Antenna Theory, Analysis and Design*, 3rd Edition, John Wiley & Sons, 2010.

14. Prasad, K. D., *Antenna Wave and Propagation*, Satya Parkashan, 1983.

15. Shakib, M. N., M. Moghavvemi, and W. N. L. Mahadi, "A low profile patch antenna for ultra-wide band application," *IEEE Letters Antenna and Wireless propagation*, Vol. 14, 1790–1793, 2015.

16. Liu, Q., J. Shen, J. Yin, H. Liu, and Y. Liu, "Compact 0.92/2.45-GHz dual-band directional circularly polarized microstrip antenna for handheld RFID reader applications," *IEEE Transactions on Antenna and Propagation*, Vol. 63, No. 9, 3849–3856, 2015.

17. Li, M. and K.-M. Lu, "A low-profile, low-backlobe and wideband complementary antenna for wireless application," *IEEE Transactions on Antennas and Propagation*, Vol. 63, No. 1, 7–14, 2015.

18. Yao, Y., S. Liao, J. Wang, K. Xue, E. A. Balfour, and Y. Luo "A new patch antenna designed for CubeSat: Dual feed, L/S dual-band stacked, and circularly polarized?," *IEEE Journals & Magazines on Antenna and Propagation*, Vol. 58, No. 3, 16–21, 2016.

19. Nasimuddin, N., Z. N. Chen, and X. Qing, "Bandwidth enhancement of a single-feed circularly polarized antenna using a metasurface," *IEEE Magazine on Antennas & Propagation*, Vol. 58, No. 2, 39–46, 2016.

20. Van Rooyen, M., J. W. Odendaal, and J. Joubert, "High-gain directional antenna for WLAN and WiMAX applications," *IEEE Letters on Antennas and Wireless Propagation*, Vol. 16, 286–289, 2017.

21. Dong, J., X. Yu, and L. Deng, "A decoupled multiband dual-antenna system for WWAN/LTE smartphone applications," *IEEE Letters on Antennas and Wireless Propagation*, Vol. 16, 1528–1532, 2017.

22. Wei, K., J. Y. Li, L. Wang, R. Xu, and Z. J. Xing, "A new technique to design circularly polarized microstrip antenna by fractal defected ground structure," *IEEE Transactions on Antennas and Propagation*, Vol. 65, No. 7, 3721–3725, 2017.

23. Choukiker, Y. K. and S. K. Behera, "Wideband frequency reconfigurable Koch snowflake fractal antenna," *IET Microwave Antennas Propagation*, Vol. 11, No. 2, 203–208, Feb. 2017.

24. Biswas, B., R. Ghatak, and D. R. Poddar, "A fern fractal leaf inspired wideband antipodal Vivaldi antenna for microwave imaging system," *IEEE Transactions Antennas Propagation*, Vol. 65, No. 11, 6126–6129, Nov. 2017.

25. Arif, A., M. Zubair, M. Ali, M. U. Khan, and M. Q. Mehmood, "A compact, low-profile fractal antenna for wearable on-body WBAN applications," *IEEE Antennas and Wireless Propagation Letters*, Vol. 18, No. 5, 981–985, May 2019.

26. Wei, K., B. Zhu, and M. Tao, "The circular polarization diversity antennas achieved by a fractal defected ground structure," *IEEE Access*, Vol. 7, 92030–92036, 2019.

27. Wang, Z., J. Liu, and Y. Long, "A simple wide-bandwidth and high-gain microstrip patch antenna with both sides shorted," *IEEE Antennas and Wireless Propagation Letters*, Vol. 18, No. 6, 1144–1148, June 2019.

28. Velan, S., E. F. Sundarsingh, M. Kanagasabai, A. K. Sarma, C. Raviteja, R. Sivasamy, and J. K. Pakkathillam, "Dual-band EBG integrated monopole antenna deploying fractal geometry for wearable applications," *IEEE Antennas Wireless Propagation Letters*, Vol. 14, 249–252, 2015.

29. Agneessens, S., S. Lemey, T. Vervust, and H. Rogier, "Wearable small and robust: The circular quarter-mode textile antenna," *IEEE Antennas Wireless Propagation Letters*, Vol. 14, 1482–1485, 2015.

30. Gupta, A., H. Dutt, and R. Khanna, "An X-shaped fractal antenna with DGS for multiband applications," *International Journal of Microwave and Wireless Technologies*, Vol. 9, No. 5, 1075–1083, 2017.

31. Hu, Z., W. Xin, Y. Luo, Y. Hu, and Y. Zhou, "Design of a modified circular-cut multiband fractal antenna," *The Journal of China Universities of Posts and Telecommunications*, Vol. 23, No. 6, 68–75, Science Direct Elsevier, 2016.

32. Benyetho, T., J. Zbitou, L. El Abdellaoui, H. Bennis, and A. Tribak, "A new fractal multiband antenna for wireless power transmission applications," *Hindawi Active and Passive Electronic Components*, Vol. 2018, 1–10, 2018.